Conf-750465--1

Radionuclide Computerized Tomography for Brain Study

David E. Kuhl, Roy Q. Edwards, Abass Alavi,
Martin Reivich, and Howard Rothenberg

Department of Radiology,
Hospital of the University of Pennsylvania,
Philadelphia, Pennsylvania

Presented At The Workshop On
Reconstruction Tomography In Diagnostic Radiology
In Nuclear Medicine

18 April, 1975, San Juan, Puerto Rico

NOTICE

This report was prepared as an account of work sponsored by the United States Government. Neither the United States nor the United States Energy Research and Development Administration, nor any of their employees, nor any of their contractors, subcontractors, or their employees, makes any warranty, express or implied, or assumes any legal liability or responsibility for the accuracy, completeness or usefulness of any information, apparatus, product or process disclosed, or represents that its use would not infringe privately owned rights.

MASTER

DISTRIBUTION OF THIS DOCUMENT UNLIMITED

Radionuclide Computerized Tomography for Brain Study

In our earlier studies (1-3) we concluded that brain scanning with ^{99m}Tc pertechnetate was complemented by transverse section scanning which enhanced detection and separation of lesions, especially near the base of the brain. With the introduction of x-ray CT (4,5) there is renewed interest in how radionuclide CT can complement these studies and how the method may be exploited to give new kinds of physiologic data. This is a brief review of some of our results and directions in this type of brain study.

MARK III System

The radionuclide CT scans shown in this paper were obtained on our MARK III scanning system (6) which has been in use for about five years. The scanner has four 2-in. diameter x $\frac{1}{2}$-in. thick NaI (Tl) detectors with focused collimators. It has been used primarily in scanning ^{99m}Tc or ^{111}In. The index of resolution (fwhm) is approximately 1.3 cm for 140 kev photons.

In a typical examination, four conventional rectilinear views of the brain are first obtained by a combination of linear scan motion of the four detectors while indexing the patient stepwise through the scanner between scan lines. These pictures are then generated on a cathode-ray tube (CRT) for interpretation. The physician reviews the scans and selects a scan line on the display for section scanning.

The section scan mode is illustrated in Figure 1. The transverse section scan is a series of six linear scans at 15^0 increments around the head. A transverse section scan requires 5-20 minutes for completion with this instrument. In the more recent use of device, section scan data are first recorded on perforated paper tape, reconstructed to a 64 x 64 matrix by an additive tangent correction method and finally displayed on the CRT for interpretation.

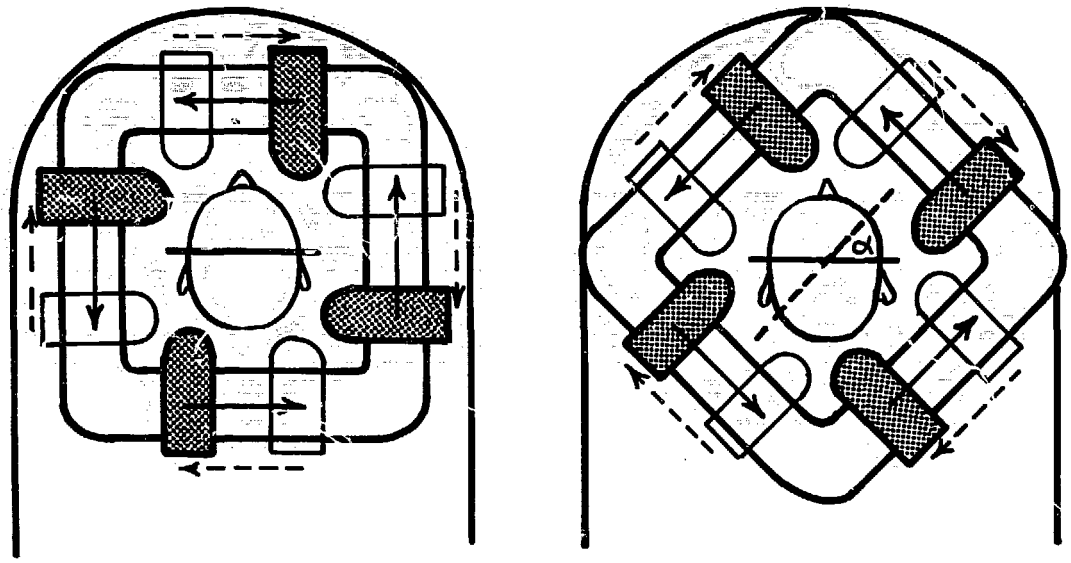

FIGURE 1: Scanning mode of the MARK III System.

Scan Examples

Figures 2 and 3 demonstrate the complementary nature of x-ray CT brain scans[1] and radionuclide CT brain scans made using ^{99m}Tc pertechnetate.

The patient whose scans are shown in Figure 2 has multiple brain metastases from lung carcinoma. The x-ray CT scan made without contrast media is abnormal (A), but the separate lesions are enhanced in the scan obtained after intravenous injectio of Conray 60 (B). The radionuclide CT scan demonstrates the same lesions with clarity Probably the mechanism for concentration of Conray in these lesions is the same as for the concentration of ^{99m}Tc pertechnetate, i.e., penetration of an altered blood-brain-barrier in the tumors.

The patient whose scans are shown in Figure 3 has an intracerebral hematoma involving the region of the internal capsule, posterior limb, and posterior part of the putamen. The x-ray CT scan made without injection of contrast (A) shows the dense central hematoma. The radionuclide CT scan shows uptake only in a ring around the hematoma, probably representing increased uptake in infarcted tissue next to the hematoma.

We have also used radionuclide CT to separate and define more clearly the anaton of cerebral spinal fluid cisterns in radionuclide cisternography (7). Figure 4 shows the normal anatomy of the basal cisterns in a series of section scans made after the subarachnoid injection of ^{111}In-DTPA. In conventional images, these cisterns are difficult to distinguish. Note that these very thin spaces are shown with surprising detail in these sections, even though the spatial resolution of this scanning system is large (fwhm = 1.3 cm) compared to their dimensions. But the differential concentr ion is high between radioactive cerebral spinal fluid and adjacent brain and relativ small distortions of distribution can be demonstrated in the radionuclide CT scan.

---

1. EMI Scanner with 160 x 160 matrix.

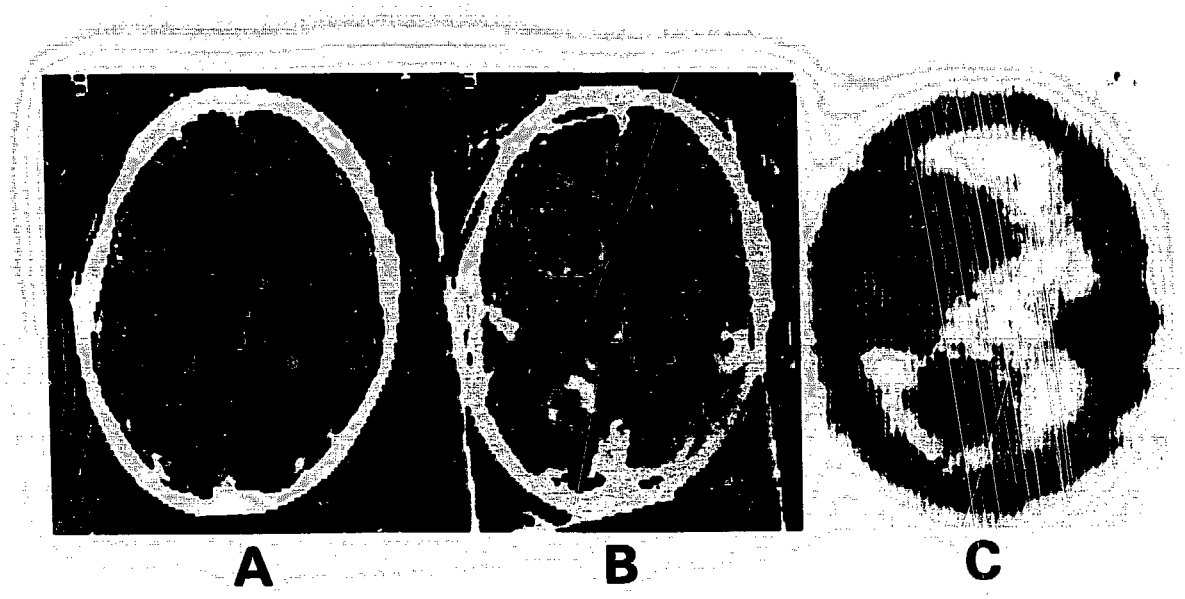

FIGURE 2: Patient with cerebral metastases shown in (A) x-ray CT without contrast injection, (B)x-ray CT with contrast injection, and (C) radionuclide CT (^{99m}Tc pertechnetate).

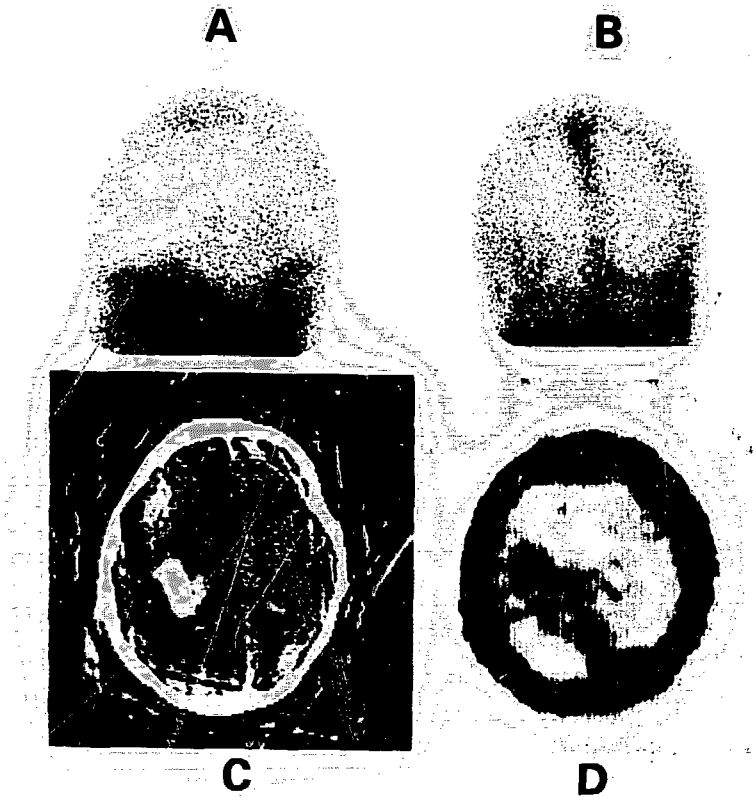

FIGURE 3: Patient with intracerebral hematoma. A and B are conventional scintillation camera images (^{99m}Tc pertechnetate) X-ray CT without contrast injection demonstrates dense hematoma (C) while radionuclide CT (^{99m}Tc pertechnetate) shows uptake in infarcted ring of tissue about the hematoma (D).

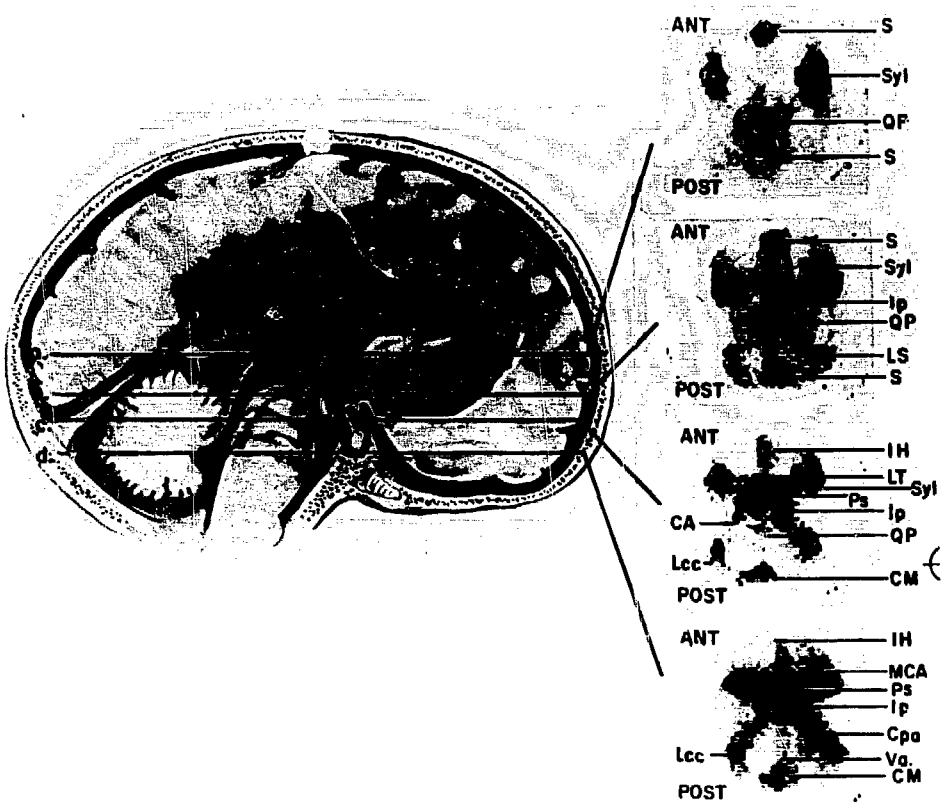

FIGURE 4: The transverse section anatomy of the normal basal cisterns. The level of each transverse section is shown by the horizontal line in the accompanying diagram. Abbreviation: (CA) cisterna ambiens, (CM) cisterna magna, (Cpa) cerebellopontine angle, (IH) interhemispheric, (Ip) interpeduncular, (Lcc) lateral cerebellar, (LS) lateral sinus, (LT) Lamina terminalis, (MCA) middle cerebral artery cistern, (Ps) paraseller cisterns, (QP) quadrigeminal plate cistern, (D) parasaggital, (Syl) Sylvian cistern, (Va) vallecula.

Quantitative Physiologic Studies

Recent advances in the development of reconstruction algorithms for radionuclide CT scanning have made it possible to obtain digital representations of the section image which are quantitatively related to radionuclide content (8-11). In our work we have used tangent correction processes for reconstruction (12,13), first a multiplicative correction designated Orthogonal Tangent Correction (OTC)(8), and now an additive correction process designated Cumulative Additive Tangent Correction (CATC). After reconstruction of the emission image from counting data, we make an approximate correction for attenuation by multiplying all values in the matrix by a factor the value of which depends on the position of each picture element. These factors are determined from a scan of a cylinder of radioactive water (Fig 5). The correction assumes the patient's head is symmetrical, centered in the scan field, and has the same attenuation properties as water. Our experience has been that this method of correction succeeds quite well for regions beneath the skull. We estimate that we can predict radionuclide concentration within a 2-cm diameter region to within a 6% coefficient of variation (14).

We have employed quantitative radionuclide CT for the study of local cerebral blood volume (LCBV)(14). Measurement of LCBV in patients would be useful for assessing cerebral hemodynamics. Changes in LCBV are known to occur in physiologic states such as mentation (15), sleep (16), with alteration of arterial CO_2 tension (17), and in pathologic states such as increased intracranial pressure (18). However, accurate measurement of LCBV in vivo is difficult. Techniques employing external radionuclide counting are complicated by interference from radionuclide concentrations in the overlying scalp and cranium (19) and often require intra-arterial injections.

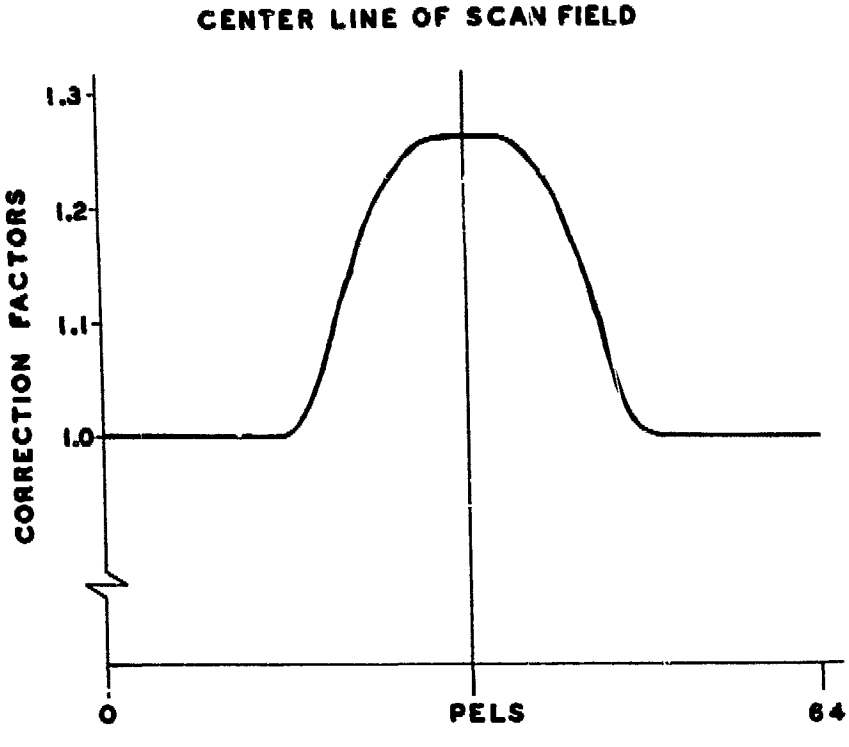

FIGURE 5: Experimentally determined factors for approximate correction for attenuation after reconstruction of section scan data.

The method requires an injection of labelled (^{99m}Tc) red cells into a peripheral vein followed by section scanning of the brain. During the scan, a blood sample is taken and the activity in red cells and in plasma determined. Counting data from scanning are reconstructed and corrected to represent region-to-region concentration of radioactivity in a cross-section of the brain. The measured concentration of blood radioactivity is used to convert the brain activity to LCBV expressed in ml blood/100 g of brain tissue. The result is a two-dimensional map of LCBV which represents a cross-section of the brain at a known level.

In a series of four baboons, we found good agreement between the section scan results and the results from in vitro counting of brain samples; the coefficient of variation of the data was 6.7% for brain activity concentration and 8.1% for LCBV. The reproducibility of the scan method was estimated over a time period of several hours in an animal maintained in a steady state. The mean of the scan-determined LCBV values for a two cm square in the center of the brain was 3.22 ml blood/100 g with a coefficient variation of 6.5%. In a series of five baboons, the following equation was obtained for the regression plane which relates LCBV in the center ofthe brain to P_aCO_2 and mean arterial blood pressure (MABP).

$$LCBV = 2.88 + 0.049\ P_aCO_2 - 0.013\ MABP$$

These data agree well with the few similar results known from the literature (Table 1).

Figure 6 shows the normalized regression plane A for scan-determined LCBV and the corresponding plane B for external counting data which were obtained without benefit of section reconstruction. Note the disparity in slopes. External counting without section reconstruction is an insensitive indicator of CBV, as would be expected, since there is no discrimination against the effect on the data of extra-cerebral circulation.

TABLE 1: Response of LCBV measured by radionuclide CT to P_aCO_2 and mean arterial blood pressure (MABP) and comparison to previous work.

ANIMAL	P_aCO_2 Slope	MABP Slope	References
Goat	0.043		Smith et al, 1971 (17)
Rhesus Monkey	0.049		Phelps et al, 1973 (20)
Rhesus Monkey		-0.015	Grubb et al, 1973 (21)
Baboon	0.049	-0.013	This work (14)

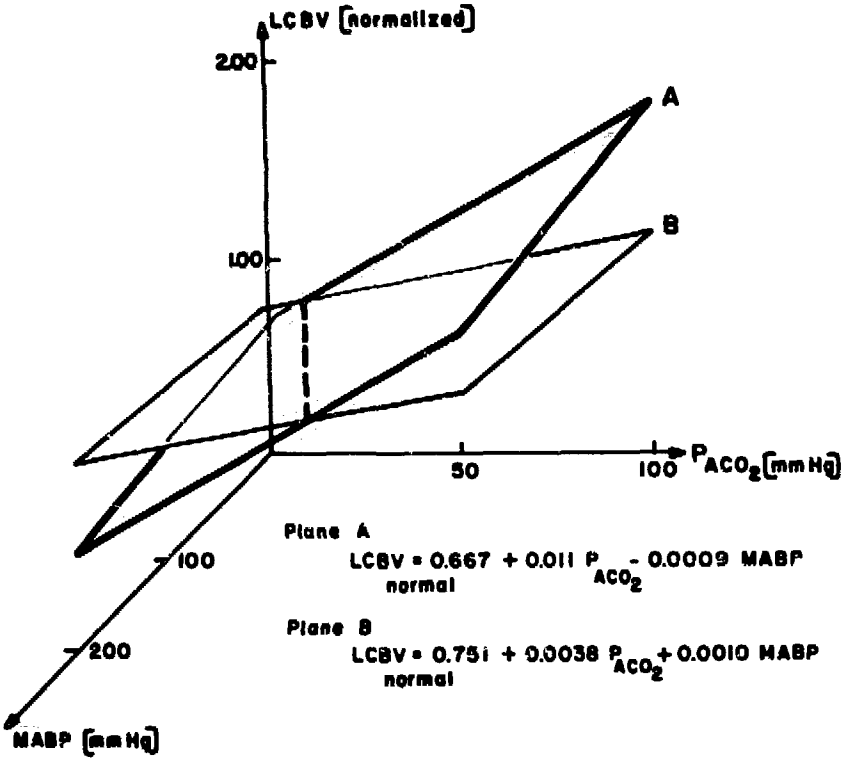

FIGURE 6: Response of CBV to P_aCO_2 and MABP. The slopes are different for the two normalized regression planes (plane A-external counting data with section reconstruction and plane B-external counting data without section reconstruction). The MABP slope of plane B is opposite in sign to what would be expected with autoregulation. External counting without section reconstruction is an insensitive indicator of CBV.

In patients, LCBV values range from 2-4 ml/100 g depending on location, with higher values corresponding to regions of cerebral cortex. An example of an LCBV scan is shown in Figure 7. In this instance, a brain tumor was found to have an LCBV significantly greater than the adjacent normal brain. In other instances, the tumor may have an LCBV lower than normal, especially in adjacent regions where the local microcirculation is compressed by edema.

MARK IV System

We have now completed and are testing the MARK IV system (Fig 8) which was designed to be at least ten times more sensitive than the MARK III instrument. The device uses a continuously rotating set of 4-collimated detector arrays. Each array is comprised of a linear arrangement of eight NaI (Tl) detectors measuring 3-in. high x 1-in. wide x 1-in. thick. The 32 detectors are arranged as a box surround the brain. Each individual detector is comprised of a separate collimator, crystal, light pipe, photo multiplier tube, and pulse height analyzer. The collimators are designed to provide an index of resolution (fwhm) of approximately 1.3 cm in the scan field.

The center-to-center distance of detectors is 3.2 cm. The position of each array is displaced linearly by .8 cm compared to each neighboring array. By interlacing data from corresponding detectors after one complete revolution, a tangent line of data is caused to contain 32 tangent elements, each .8 cm wide.

The four detector arrays are attached to a large hollow square axle which enclose data reduction electronics. As the detector square rotates, data are collected continuously, processed in the individual pulse-height analyzers, and introduced to 32 counters mounted in the axle. These data are then passed through shift registers at intervals of 2.5^0 of rotation and then through an optical channel to a mini-compute The 32 channels of data are then batched into increments of 7.5^0 of rotation an

1. Texas Instrument 980A.

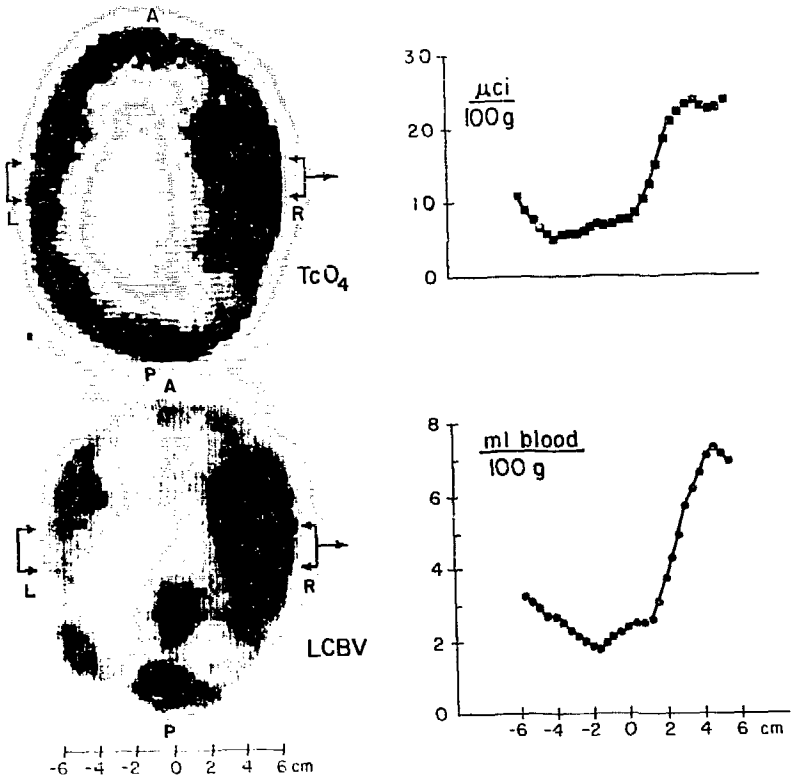

FIGURE 7: Section scans of a malignant glioma previously thought to be cerebral infarct. Section scan of ^{99m}Tc per echnetate (top left) demonstrates local alteration in blood brain barrier and section scan of ^{99m}Tc red cells (bottom left) demonstrates local cerebral blood volume. Corresponding quantitative data are shown at the right. The lesion had three times the normal blood volume. At autopsy the tumor was found to be much more highly vascular than the adjacent normal brain.

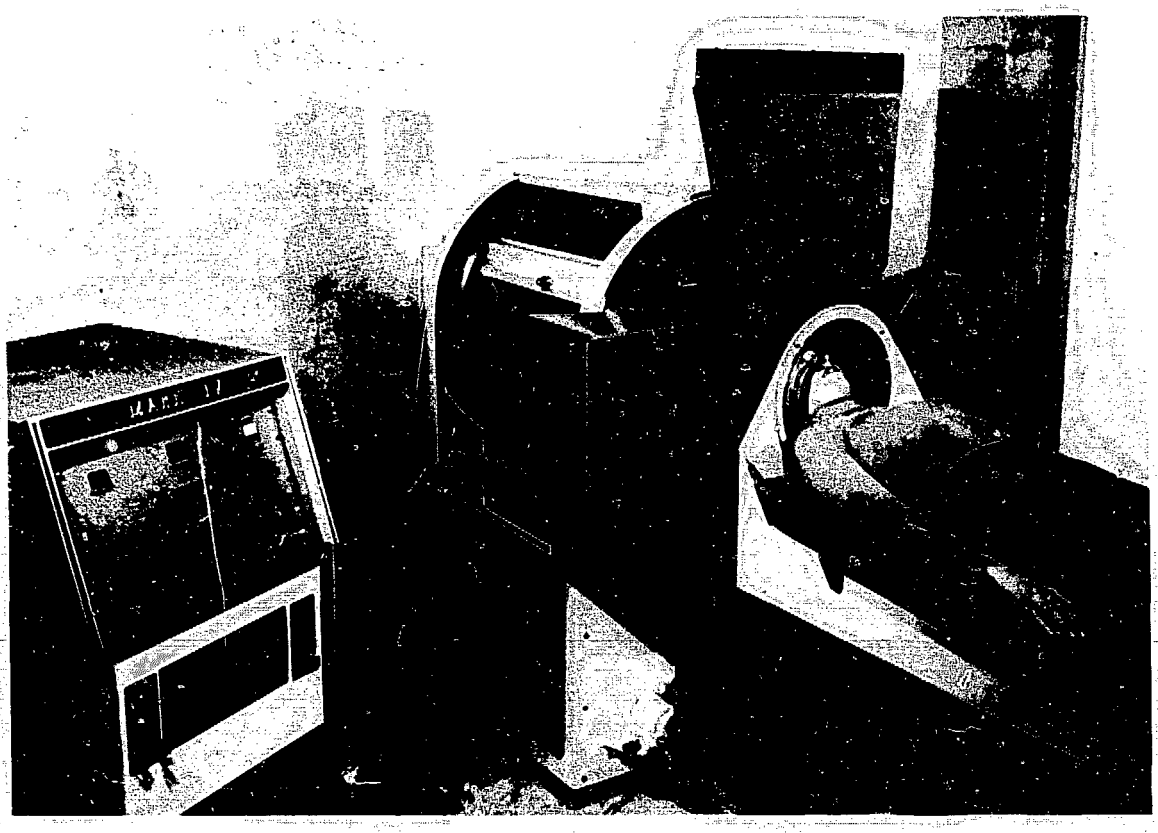

FIGURE 8: MARK IV system now undergoing testing.

until completion of the full detector revolution of 360^0. Then the accumulated data are transferred to a digital computer[1] for reconstruction processing.

Next the data are corrected to equal detector response among the 32 detectors using data from counting a source prior to the study. In each tangent line, the 32 tangent elements are expanded by linear interpolation to produce 64 tangent elements. The reconstruction method is an additive correction process[12,13] performed on each tangent line of data at 7.5^0 angular intervals in orthogonal sequence. This requires 30 seconds for completion, whereupon the reconstructed matrix from a single revolution outputs to a core store and is displayed on a CRT.

Meanwhile, the detectors continue to rotate and a new set of data is built-up in the preprocessor. After completion of the next revolution, a new set of counting data, comprised of the previous plus the new counting data is introduced to the computer processed against the reconstructed matrix, and outputed to the display. In this way, the new data from each revolution are added to the previous data and reprocessed for a new picture, the final reconstructed matrix being stored in disc memory.

Since the instrument operates at 50 seconds per revolution, the continuous collection and processing of data causes a new picture to appear on the display every 50 seconds as the study progresses. The duration of the examination may be extended or curtailed by the operator according to the appearance of the picture.

Discussion

Accurate knowledge of regional function in the brain would be of great value for the detection and localization of a wide variety of diseases and for assessment

---

1. Varian 620/i

of patients under treatment. The management of patients would be greatly improved with a day-to-day knowledge of the status of blood flow, blood volume, metabolism, permeability, brain swelling and other functions on a local basis throughout the brain. In the past this kind of information has not been available. Instead, function has usually been examined only for the organ as a whole and regional information has been restricted to morphology as determined by radiographic or radionuclide imaging studies. Three-dimensional radionuclide reconstruction imaging will become more important in the study of the brain, providing accurate measurement of radionuclide concentration within functional structural units of the brain. Measurement of local function with three-dimensional resolution throughout the brain and without the necessity for intra-carotid injection of indicator could therefore provide a significant advance over presently available methods.

Acknowledgement

This work was supported in part by USPHS Research Grant 2R01 GM-16248, USAEC Contract AT(11-1)-3399, USPHS Program Project Grant 5P01NS-10930, and USPHS Research Career Development Award 2-KS-HS-11 (M.R.)

REFERENCES

1. Kuhl, D.E., and Edwards, R.Q.: Image Separation Radioisotope Scanning. Radiology 80: 653-662, April 1963.

2. Kuhl, D.E., Pitts, F.W., Sanders, T.P., and Mishkin, M.M.: Transverse Section and Rectilinear Brain Scanning Using ^{99m}Tc pertechnetate. Radiology 86: 822-829, May 1966.

3. Kuhl, D.E., and Sanders, T.P.: Characterizing Brain Lesions Using Transverse Section Scanning. Radiology 98: 317-328, Feb. 1971.

4. Hounsfield, G.N.: Computerized Transverse Axial Scanning (Tomography): Part I. Description of System. British Journal of Radiology 46: 1016-1022, Dec 1973.

5. Ambrose, J.: Computerized Transverse Axial Scanning (Tomography): Part 2: Clinical Application. British Journal of Radiology 46: 1023-1047, Dec 1973.

6. Kuhl, D.E. and Edwards, R.Q.: The MARK III Scanner: A Compact Device for Multiple-View and Section Scanning of the Brain. Radiology 96: 563-570, Sept 1970.

7. Rothenberg, H.P., Devenney, J., and Kuhl, D.E.: Transverse Section Radionuclide Cisternography. (In press)

8. Kuhl, D.E., Edwards, R.Q., Ricci, A.R., and Reivich,M.:Quantitative Section Scanning Using Orthogonal Tangent Correction. J. Nucl Med 14: 196-200, April, 1973.

REFERENCES

9. Budinger, T.F., and Gullberg, T.T.: Three-Dimensional Reconstruction In Nuclear Medicine By Iterative Least-Squares and Fourier Transform Techniques. USAEC Report LBL-2146, TID-4500-R61, Jan 1974.

10. Ter-Pogossian, M.M., Phelps, M.E., Hoffman, E.J., and Mullani, N.A.: A Positron-Emission Transaxial Tomography for Nuclear Imaging (PETT). Radiology 114: 89-98, Jan 1975.

11. Phelps, M.E., Hoffman, E.J., Mullani, N.A., and Ter-Pogossian, M.M.: Application of Annihilation Coincidence Detection to Transaxial Reconstruction Tomography. J. Nucl Med 16: 210-224, March, 1975.

12. Gordon, R., Bender, R. and Herman, G.T.: Algebraic Reconstruction Techniques (ART) for Three-Dimensional Electron Microscopy and X-ray Photography. J. Theor Biol. 29: 471, 1970.

13. Gilbert, R.: Iterative Methods for the Three-Dimensional Reconstruction of an Object from Projections. J. Theor. Biol. 36: 105, 1972.

14. Kuhl, D.E., Reivich, M., Alavi, A., Nyary, I., and Staum, M.M.: Local Cerebral Blood Volume Determined by Three-Dimensional Reconstruction of Radionuclide Scan Data, Circulation Research.(In press)

15. Risberg, J. and Ingvar, D.H.: Regional Changes in Cerebral Blood Volume during Mental Activity. Exp. Brain Research 5: 72-78, 1968.

REFERENCES

16. Risberg, J., Gustavsson, L., and Ingvar, D.H.: Regional Cerebral Blood Volume during Paradoxical Sleep. In: Brock, M., Fieschi, C., Ingvar, D.H., Lassen, N.A., and Schurmann, K. (eds) Cerebral Blood Flow. Clinical and Experimental Results. Springer, Berlin, pages 101-103, 1969.

17. Smith, A.L., Neufeld, J.R., Ominsky, A.J., and Wollman, H.: Effect of Arterial CO_2 Tension of Cerebral Blood Flow, Mean Transit Time, and Vascular Volume. J. Appl. Physiol. 31: 701-707, 1971.

18. Langfitt, T.W., Weinstein, J.D., and Hassell, N.F.: Cerebral Vasomotor Paralysis Produced by Intracranial Hypertension. Neurology 15: 662-643, 1965.

19. Oldendorf, W.H. and Lisaka, Y.: Interference of Scalp and Skull with External Measurements of Brain Isotope Content: Part I Isotope Content of Scalp and Skull. J. Nuc Med 10: 177-183, 1969.

20. Phelps, M.E., Grubb, R.L., and Ter-Pogossian, M.M.: Correlation Between P_aCO_2 and Regional Cerebral Blood Volume by X-ray Fluorescence. J. Appl. Physiol. 35: 274-280, Aug 1973.

21. Grubb, R.L., Jr., Phelps, M.E., Raichle, M.E., and Ter-Pogossian, M.M.: The Effects of Arterial Blood Pressure on the Regional Cerebral Blood Volume By X-ray Fluorescence. Stroke, 4: 390-399, 1973.

ILLUSTRATIONS

Figure 1: Scanning mode of the MARK III System.

Figure 2: Patient with cerebral metastases shown in (A) x-ray CT without contrast injection, (B) x-ray CT with contrast injection, and (C) radionuclide CT (^{99m}Tc pertechnetate).

Figure 3: Patient with intracerebral hematoma. A and B are conventional scintillation camera images (^{99m}Tc pertechnetate). X-ray CT without contrast injection demonstrates dense hematoma (C) while radionuclide CT (^{99m}Tc pertechnetate) shows uptake in infarcted ring of tissue about the hematoma (D).

Figure 4: The transverse section anatomy of the normal basal cisterns. The level of each transverse section is shown by the horizontal line in the accompanying diagram. Abbreviation: (CA) cisterna ambiens, (CM) cisterna magna, (Cpa) cerebellopontine angle, (IH) interhemispheric, (Ip) interpeduncular, (Lcc) lateral cerebellar, (LS) lateral sinus, (LT) lamina terminalis, (MCA) middle cerebral artery cistern, (Ps) parasellar cisterns, (QP) quadrigeminal plate cistern, (S) parasaggital, (Syl) Sylvian cistern, (Va) vallecula.

ILLUSTRATIONS

Figure 5: Experimentally determined factors for approximate correction for attenuation after reconstruction of section scan data.

Figure 6: Response of CBV to P_aCO_2 and MABP. The slopes are different for the two normalized regression planes (plane A-external counting data with section reconstruction and plane B-external counting data without section reconstruction). The MABP slope of plane B is opposite in sign to what would be expected with autoregulation. External counting without section reconstruction is an insensitive indicator of CBV.

Figure 7: Section scans of a malignant glioma previously thought to be cerebral infarct. Section scan of ^{99m}Tc pertechnetate (top left) demonstrates local alteration in blood brain barrier and section scan of ^{99m}Tc red cells (bottom left) demonstrates local cerebral blood volume. Corresponding quantitative data are shown at the right. The lesion had three times the normal blood volume. At autopsy the tumor was found to be much more highly vascular than the adjacent normal brain.

Figure 8: MARK IV system now undergoing testing.

Figures 1, 2, and 3 in this paper are included in a manuscript entitled, "Emission Computerized Transaxial Tomography and Determination of Local Brain Function" by D.E. Kuhl et al, which has been accepted for publication in the proceedings of the symposium "Past, Present, and Future of Non-Invasive Brain Imaging", Salt Lake City, Utah, 19 February, 1975, which is to be published by the Society of Nuclear Medicine.

Figure 4 is an illustration in reference 7 and is currently in press with RADIOLOGY.

Figures 6 and 7 are from reference 14 which has been accepted for publication by CIRCULATION RESEARCH.

David E. Kuhl, M.D.
16 April, 1975